Chapter 8

Global Detectors

In addition to the two small solid-angle spectrometers, BRAHMS will employ beam-beam counters and a centrality detector to characterize collisions from a global perspective and to form zero and first level triggers. The beam-beam counters will provide the start time for the time-of-flight measurements as well as determining the vertex position to an accuracy of order 1 cm. The centrality detector will measure the centrality ("impact parameter") of collisions by recording a related quantity, the charged particle multiplicity at midrapidity; additional information from the beam-beam counters complements this coverage.

8.1 Beam-Beam Counters

The BRAHMS beam-beam counters will consist of two arrays of Čerenkov detectors with one array located on each side of the intersection region as is shown in the detail of Fig. 5.1. These counters will provide the start timing for time-of-flight measurements, sample $dn/d\eta$ at high η, and provide initial vertex determination. Similar systems have been discussed for the other RHIC experiments. In this section we will discuss the design parameters for the BRAHMS Experiment.

The design constraints of the beam-beam counter system for BRAHMS are dominated by the need for a good timing start for the spectrometers. The detector modules are designed to detect the Čerenkov light from $\beta = 1$ charged particles. Placement of the counters in a region of high η ensures that most of the particles have β near 1, enabling an array with a reasonable number of modules to efficiently provide a timing start. Each module will consist of a lucite radiator attached to a good timing photomultiplier. The radiator must be sufficiently thick (2-4 cm), such that a $\beta = 1$ charged particle will have a timing resolution of 50 ps. Multiple particles striking a single module may compromise the ability to provide good timing. Estimates of 10 hits per module for central Au+Au collisions have been considered for various system designs, where the region of pseudo-rapidity is spanned by only a small number of counters. To avoid this potential problem, we will sparsely sample a region of η ensuring that several counters have only one or two hits for the most central events. For a fixed number of counters, sparse sampling has the disadvantage of introducing an inefficiency at lower multiplicities. We will illustrate this with a preliminary detector layout.

Fig. 8.1 shows the front view of the two beam counter arrays. The left array has 40 modules sampling η from 3.0 to 4.5. The right array has 35 modules and samples the opposite η region but with reduced azimuthal coverage since magnet D1 is on the opposite side of the beam pipe. A higher spatial density of modules has been used in the right array to partially compensate for the reduced azimuthal coverage. The dots shown in Fig. 8.1 represent the expected charged particle hit density. Four different module sizes are used in the arrays. The larger modules use a two-inch Hamamatsu fast timing tube (R2083) with either 2- or 2.5-inch diameter lucite radiators. The smaller modules use a 0.75-inch diameter Hamamatsu tube with lucite radiators of diameter 0.75 or 1.0 inches. Prototypes of these modules will be tested to ensure that they provide the desired 50 ps timing resolution. The array-geometry will later be refined based on the results of the prototype tests.

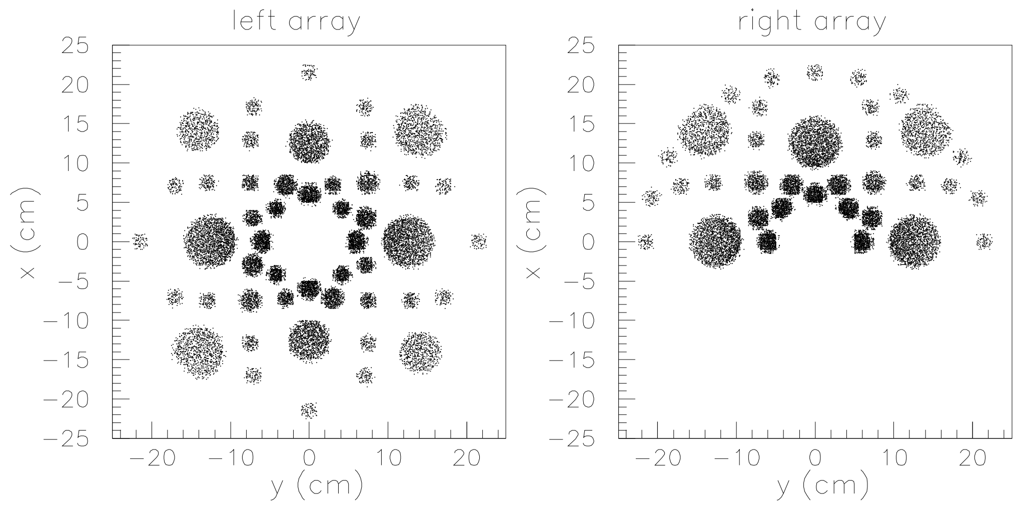

Figure 8.1: Schematic view of the two beam-beam counter arrays. The points represent charged particles striking the active area of the modules. Central Au+Au collisions from FRITIOF have been parameterized to simulate the hit density.

An estimate of the efficiency with which the combined array can provide a good

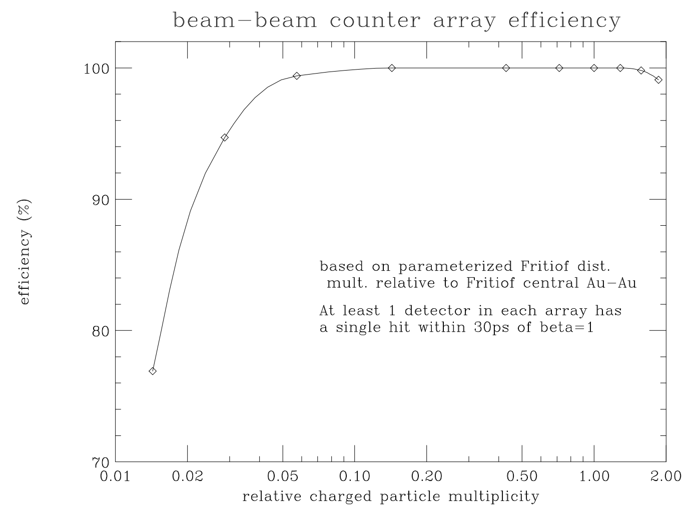

Figure 8.2: Efficiency of the beam-beam array to provide a good timing start as a function of relative multiplicity. Central Au+Au collisions from FRITIOF correspond to a relative multiplicity of 1.

timing start has been made. The charged particle distributions for Au+Au central collisions from FRITIOF have been parameterized. A module is considered to produce good timing if only one charged particle strikes the active area of the module and it arrives within 30 ps of the arrival time expected for $\beta = 1$. In addition, it is required that both arrays have at least one good timing hit. The efficiency as a function of the charged particle multiplicity relative to Au+Au central events of FRITIOF is presented in Fig. 8.2. The array is nearly 100% efficient for relative multiplicities of 0.05 to 1.6. The inefficiency at lower multiplicities is a consequence of the small number of counters and sparse sampling. The inefficiencies at large relative multiplicities is the result of all modules having multiple hits for some events. Backgrounds will produce spurious hits in the arrays which will increase the occupancy. Preliminary simulations using GEANT suggest that this will only modestly affect the efficiency. These simple simulations demonstrate that a sampling array can provide an efficient start-timing over a large range of multiplicities.

8.2 Centrality detector

As mentioned above, selecting on charged particle multiplicity as a measure of the centrality ("impact parameter") of collisions will be performed by the centrality detector. The goals for this detector may be briefly stated as:

1. To use the identical detector for all systems from peripheral Si+Si to central Au+Au.
2. To provide a first-level hardware trigger for the experiment.
3. To allow an offline analysis with as many as five centrality windows for Au+Au, and at least two such windows for Si+Si.
4. To provide azimuthal angle coverage as symmetric and as complete as possible without interfering with the spectrometers.
5. To cover as large a range of pseudorapidity as possible and yet remain within a reasonable budget.

These goals guide the design of the detector in ways that are outlined below.

Silicon strip detectors have been successfully operated as vertex detectors at collider experiments[1] and are being constructed as centrality detectors for both the PHOBOS and PHENIX Experiments at RHIC[2,3]. Following the development work of these collaborations, the incremental cost per channel of such detectors is expected to be quite low, allowing a suitable device to be built for a cost of less than $250,000. In addition, it is desirable for two or more RHIC experiments to have a common centrality trigger for the purpose of comparing results. Indeed, many of the goals for the low-resolution part of the PHOBOS vertex detector coincide with those outlined above. For these reasons, BRAHMS is planning to build a silicon strip barrel detector resembling the multiplicity vertex barrel of PHOBOS.

An alternate detector technology which is also lightweight and low-cost is that of a gas proportional counter with cathode pad readout. A backup plan for a multiplicity array based on this option is outlined in a separate section below.

8.2.1 Phase-space Coverage

The total charged particle multiplicity density, $dN/d\eta$, versus pseudorapidity, η, is shown in Fig. 8.3 for central Au+Au for the two models Fritiof and Venus. Note that the two-peaked distribution for Fritiof arises not from less nucleon "stopping" in the model – protons comprise only 6% of the total multiplicity – but rather from the difference between rapidity, y, and pseudorapidity, η. Due to the inequality, $|y| \leq |\eta|$, the $dN/d\eta$ distributions are broader than the corresponding ones for dN/dy. For both Fritiof and Venus, the *shape* of the $dN/d\eta$ distribution does not depend on the mass of the projectile nor on the centrality of the collision (except for the very peripheral case), so the following argument concerning the desired coverage is appropriate within the context of these models.

A reasonable criterion for the minimum pseudorapidity coverage is to insure that both peaks in the Fritiof distribution are included. This implies covering $|\eta| \leq 2.0$, as shown

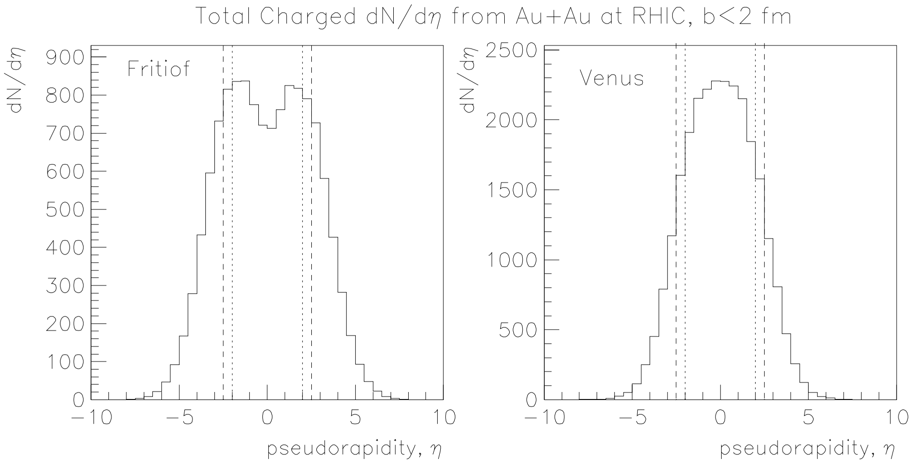

Figure 8.3: The total charged particle $dN/d\eta$ for central Au+Au. The dashed lines show coverage to ± 2.5 units of pseudorapidity, corresponding to the nominal coverage of the proposed detector; the dotted lines show the minimum coverage of ± 2.0 units.

by the dotted lines in Fig. 8.3. Note that the central peak in the Venus distribution is also well covered by this choice. For a barrel detector of radius 6 cm a pseudorapidity coverage of $|\eta| \leq 2.0$ implies a barrel length of 44 cm; however, a ± 15 cm vertex cut along the beam direction will be used in this experiment. This extra 30 cm brings the necessary total barrel length to 74 cm.

The coverage of the proposed silicon strip detector is shown in Fig. 8.4. Due to practical considerations regarding silicon wafer dimensions, the actual barrel length is 70.7 cm, implying a nominal coverage of $|\eta| \leq 2.47$ for an interaction at the diamond center. Interactions at the edge of the vertex cut give the extreme values η_{min}=1.94 and η_{max}=2.82 on opposite sides of the barrel. The barrel detector will be complemented by information from the beam-beam counters which nominally cover the pseudorapidity $3.0 \leq |\eta| \leq 4.5$.

To minimize the amount of material obscuring the apertures of the two BRAHMS spectrometers, gaps are allowed in the azimuthal coverage. As shown in the end view of Fig. 8.4, the octagonal cross-section for the barrel has six of the eight sides covered. Geant calculations with Venus central Au+Au events were used to estimate the background in the BRAHMS midrapidity spectrometer caused by the presence of the multiplicity detector silicon and associated electronics. With the spectrometer at 90°, less than one additional charged particle out of a total of 47 primary and secondary tracks was found to come from the multiplicity detector.

Figure 8.5 shows the predicted charged multiplicity distribution for a barrel detector of radius 6 cm, total length 70.7 cm and 3/4 of the azimuthal angle coverage. Effects of the vertex longitudinal position along the diamond are included, along with a ± 15

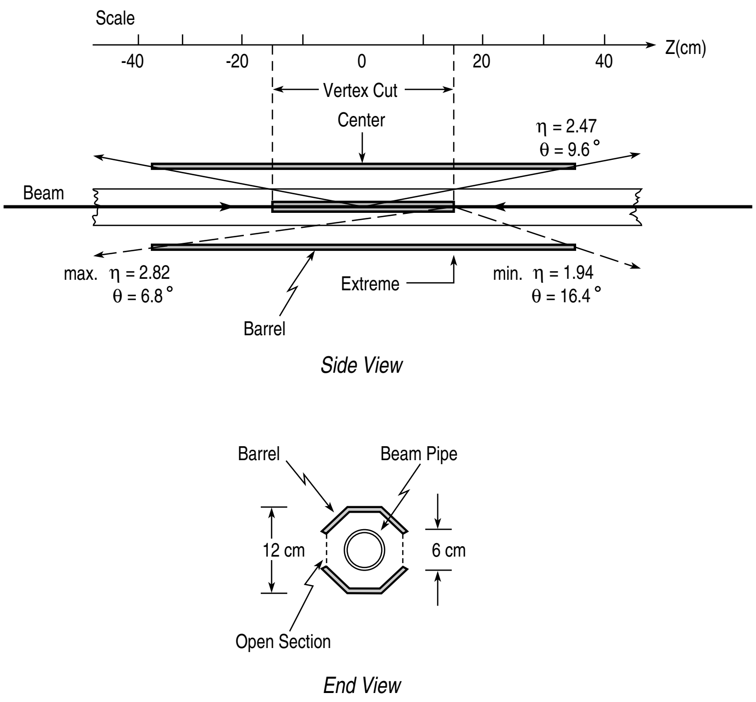

Figure 8.4: Coverage of the silicon strip multiplicity detector. The barrel has an octagonal cross-section of radius 6 cm, is 70.7 cm long, and is covered on six of the eight sides. An interaction vertex cut of ±15 cm along the beam axis will be used.

cm vertex position cut. Since it is our goal to be able to use the identical detector for measuring centrality for all systems from peripheral Si+Si to central Au+Au, a dynamic range covering multiplicities with order of magnitude from 100 to 10000 is required, as seen in Fig. 8.5. In the Au+Au case, five multiplicity windows are required for the offline analysis: this requires a resolution in the determination of multiplicity of 10% or better. For the case of Si+Si, two cuts (central and peripheral) are quite satisfactory as this projectile system will be studied mainly as a contrast to Au+Au. A different centrality detector will be needed for both p+p and p+A running.

8.2.2 Concept for a Silicon Strip Detector

The layout of the silicon strip wafers on the multiplicity detector barrel is shown in Fig. 8.6. The octagon is composed of top and bottom halves with mechanical support provided by stands on the floor; for servicing the detector and/or the beampipe, the top half may be moved up and the bottom half down, and then both may be easily removed.

The wafers are identical with Wafer Type 8 of the PHOBOS Vertex Detector[2]. Each

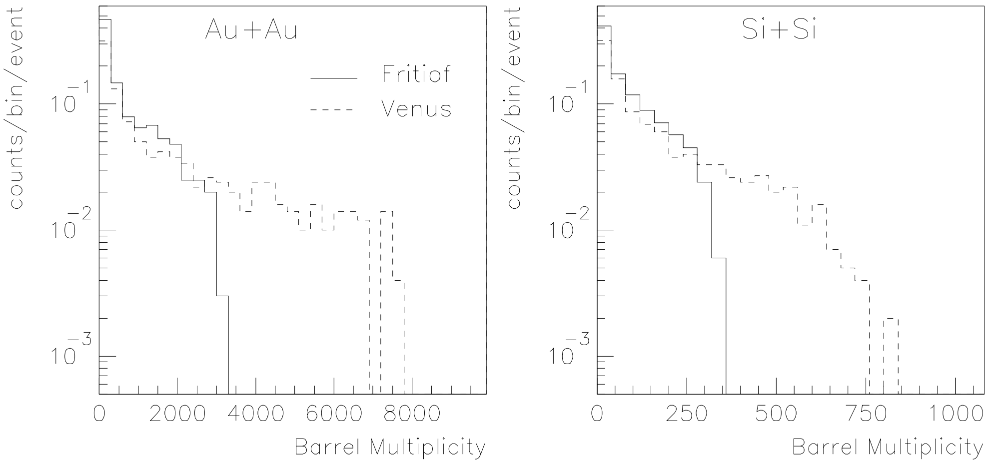

Figure 8.5: The true charged particle multiplicity distribution into a barrel with the coverage shown in Fig. 8.4, from Fritiof (solid histograms) and from Venus (dashed histograms.)

wafer is 78.6×48.8 mm^2 with an active area of 76.8×47.0 mm^2, and has 2 rows of 32 strips each (i.e., 64 strips/wafer.) Nine wafers cover the length of each side of the octagon; thus there are a total of (9 wafers/side)×(6 sides)× (64 channels/wafer) = 3456 channels. The wafer thickness is 300 μm and the strip pitch is 2.4 mm ($\Delta\eta \approx 0.05$.)

Since each silicon wafer has two sets of strips in the azimuthal direction, this implies an azimuthal segmentation of $\Delta\phi = 22.5°$ per strip. Thus the detector system will only give limited information on charged particle distributions in the azimuthal angle ϕ.

Some multi-hit capability exists with these counters and the pulse height will be recorded. The total charge from each pad is read out with ADC's and the charged-particle multiplicity is deduced from the signal and the angle of the particle trajectory from the vertex through the Si plane. Although this procedure introduces some dispersion due to variations in energy loss of the charged-particles traversing the Si wafers, it yields a multiplicity measurement which does not saturate at high multiplicities.

Monte Carlo simulations were run to gauge the expected performance of this procedure for obtaining the multiplicity. Particles from model-generated events were "thrown" one by one at the actual detector geometry, and the energy deposited in the silicon was taken from the Landau distribution appropriate for the particle's mass, velocity and thickness of silicon traversed[4]. The high-energy end of the long Landau "tail" of the distribution is comprised almost entirely of delta electrons carrying energy of order 1 MeV, or greater, and these electrons generally escape the silicon without much energy loss. This fact is accounted for in the simulations by introducing a high-energy cutoff to the Landau distribution[5]. The total energy deposited in each silicon strip was then summed for each event, including the effects of individual particles crossing more than

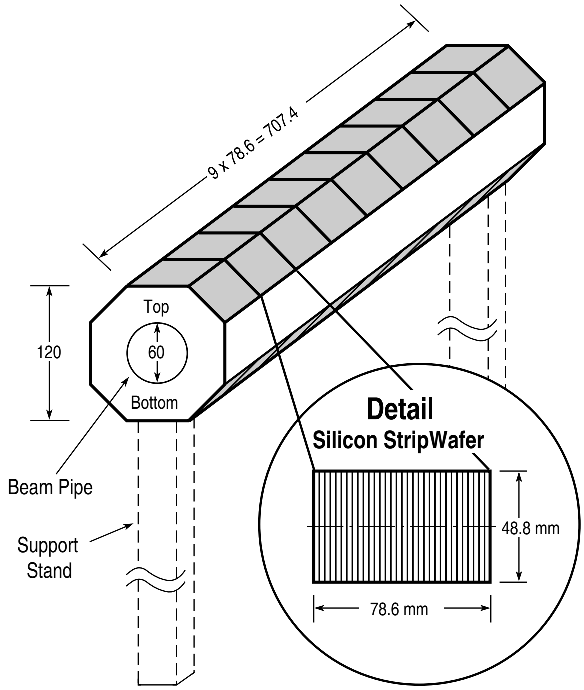

Figure 8.6: Layout of silicon wafers on the multiplicity detector barrel. Dimensions are in mm. Each wafer is 78.6×48.8 mm^2 with an active area of 76.8×47.0 mm^2.

one strip, and also including a random gaussian noise of 15 keV. (For comparison, a minimum-ionizing particle loses 116 keV in 300μm Si, on average.) In addition, a 50 keV threshold was applied for each channel. Finally, the number of particles hitting each strip was inferred, on average basis only, from the total energy deposited (in the strip) divided by the mean energy deposited per particle at that pseudorapidity. It should be noted that the mean energy deposited per particle is a model-dependent quantity which depends on the mixture of particle species produced as well as their momentum distribution.

The results of the Monte Carlo simulation described in the paragraph above are summarized in Fig. 8.7. Panel (a) plots the measured barrel multiplicity versus impact parameter for Fritiof Au+Au minimum bias events, showing the expected anti-correlation between the two quantities. In panel (b) is a histogram of the measured multiplicity for 100 trials of the same Fritiof central Au+Au event: the true charged particle multiplicity into the active barrel acceptance is 2725, whereas the mean measured value is only slightly higher at 2778. The r.m.s. width of the histogram is 22; i.e., less than 1% of the mean. Finally, panel (c) displays the measured $dN/d\eta$ for Au+Au central events from both Fritiof and Venus. The simulation with both models has been "tuned" for Fritiof in the sense that the mean energy deposited per particle (as a function of η) is derived from that model; therefore it is not too surprising that the measured $dN/d\eta$ for Fritiof is nearly identical with the input distribution. However, the fact that the measured distribution for Venus agrees with its corresponding input to $\approx 5\%$ provides confidence that the multiplicity measurement is valid in a less model-dependent manner.

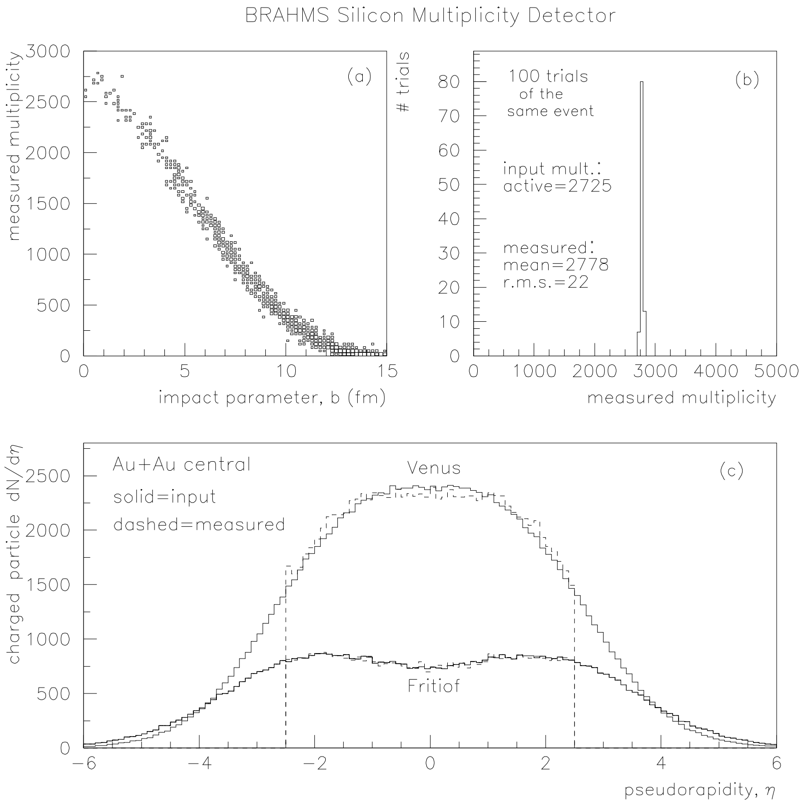

Figure 8.7: Simulated performance of the silicon strip multiplicity detector. Panel (a) shows the measured multiplicity versus impact parameter for Fritiof Au+Au events. Panel (b) shows the results of running the same Fritiof event through 100 trials. Panel (c) compares the measured $dN/d\eta$ for Au+Au central events to the inputs from both Venus and Fritiof.

The PHOBOS front-end electronics and readout, including the capability of forming an analog multiplicity trigger, would be used for BRAHMS with no changes.

The incremental cost of building this "copy" of the PHOBOS vertex detector is about \$240K.

8.2.3 The Backup Option: A Gas Proportional Counter

The option envisioned would be quite similar to the "Barrel-Section" of the Target Multiplicity Array (TMA) used successfully in E-802 at the AGS, with which members of BRAHMS have extensive experience. The basic counter element is a resistive plastic tube, 1×1 cm^2 in cross section, with a central anode wire stretched longitudinally. The gas-filled detector element is operated in the proportional mode. The particle-induced signals are read out from copper pads which form the segmented cathode plane. The read out electronics could be quite similar to that described for the original TMA, in which the barrel section had 1512 pads.

A suitable arrangement for BRAHMS would involve construction of a barrel of roughly twice the dimensions of Fig.8.4; i.e., 140 cm long and $\approx$12 cm in radius, which would cover the same range of η as illustrated. Each of the 6 flat detector planes would be comprised of 10 tubes cemented together: the length of the etched cathode pads would vary from $\approx$1 cm in the vertex region to $\approx$2-3 cm at the ends. As before, the two side sections would be open so as to not obscure the spectrometer views of the interaction diamond. The net ensemble could thus be configured to define, as desired, a segmentation range of 3000-6000 cells, and yet provide no greater scattering background than that for the silicon-strip detector described above.

With such a detector, the logic behind the determination of the experimental multiplicity is distinctly different from that of the original TMA. For TMA, the occupancy was kept low enough ($\leq$15%) such that the occurrence of multiple hits on a single element could be safely ignored. In the present case, although the occupancy is much higher, the true multiplicity may yet be determined under the assumption that the multi-hit probabilities follow pure Poisson statistics.

As an example of this approach, Fig. 8.8 summarizes the results of simple Monte Carlo calculations. For each trial, M particles were randomly thrown at $N = 5000$ channels, and from F_{hit} = fraction of channels with at least one hit, an estimate for M was deduced (M_{est}.) The mean value of F_{hit} from many trials is plotted in the figure versus the true multiplicity, M. For the multiplicity range relevant to this detector, $100 \leq M \leq 10000$, the relative r.m.s. error on the estimate, $\sigma(M_{est})/M$, is less than 1.5%. We conclude that the loss of resolution introduced by this estimating procedure, in distinction to any intrinsic detector resolution, is too small to be of concern.

8.2.4 Potential Upgrades

Possible future upgrades to the centrality detector include instrumenting more channels on the central barrel and adding endcaps to extend the pseudorapidity coverage. A separate centrality detector is necessary both for p+p and p+A running.

The more finely segmented wafers used by PHOBOS to make a precise determination of the interaction vertex ($<$ 1 mm) could also be employed for BRAHMS, albeit in a

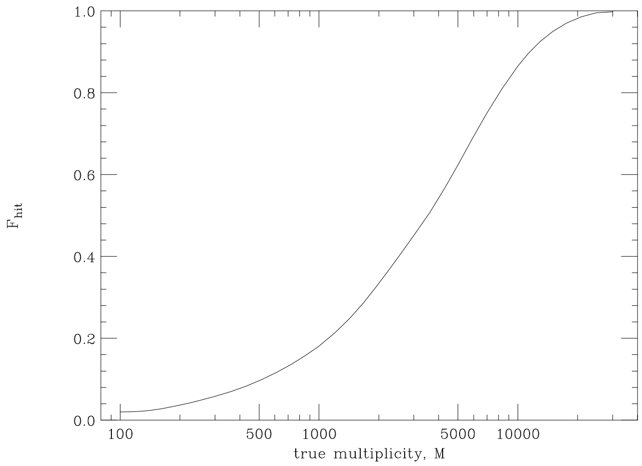

Figure 8.8: The mean fraction of channels with at least one hit as a function of the true multiplicity, M, in the acceptance of a "yes-no" detector with 5000 channels.

slightly different configuration. Two wafers, 78.6 mm $\times$ 39.8 mm^2 segmented into two rows of 0.3-mm strips, would be centered at a distance of 6 cm both above and below the beampipe. An array of 4×2 wafers of the same size, but segmented into single rows of 0.3-mm strips would be centered at a distance of 12 cm. The inner layer has a total of 1024 strips and the outer layer has a total of 2048. A precise determination of the interaction vertex will assist in a precise determination of the start-time, t_0, and in distinguishing primary tracks from secondaries in the mid-rapidity spectrometer.

8.3 References

1. For a recent review, see A.S. Schwarz, Phys. Rep. **238**, 1 (1994).
2. PHOBOS Conceptual Design Report, BNL, 1994.
3. PHENIX Conceptual Design Report, BNL, 1993.
4. A useful reference is W.R. Leo, *Techniques for Nuclear and Particle Physics Experiments*, Springer-Verlag, New York, second edition (1994).
5. The values for the cutoff derive from separate calculations which use the GEANT code. Empirically it is found that the maximum deposited energy, in keV, in 300 μm thick Si is given by $1200 + 160\eta^2$, where η is the pseudorapidity, with $|\eta| \leq 3$. This result holds whether the incident particle is a pion, kaon or proton.
6. T. Abbott, *et al.*, (E-802 Collaboration), Nucl. Instrum. Meth. **A290**, 41 (1990).